A Maximum Likelihood approach to determine sensor radiometric response coefficients for NPP VIIRS reflective solar bands

Ning Lei[1,*], Kwo-Fu Chiang[1], Hassan Oudrari[1], and Xiaoxiong Xiong[2]

1. Sigma Space Corporation, 4600 Forbes Blvd., Lanham, MD, USA 20706
2. Sciences and Exploration Directorate, NASA Goddard Space Flight Center, Greenbelt, MD, USA 20771

ABSTRACT

Optical sensors aboard Earth orbiting satellites such as the next generation Visible/Infrared Imager/Radiometer Suite (VIIRS) assume that the sensors' radiometric response in the Reflective Solar Bands (RSB) is described by a quadratic polynomial, in relating the aperture spectral radiance to the sensor Digital Number (DN) readout. For VIIRS Flight Unit 1, the coefficients are to be determined before launch by an attenuation method, although the linear coefficient will be further determined on-orbit through observing the Solar Diffuser. In determining the quadratic polynomial coefficients by the attenuation method, a Maximum Likelihood approach is applied in carrying out the least-squares procedure. Crucial to the Maximum Likelihood least-squares procedure is the computation of the weight. The weight not only has a contribution from the noise of the sensor's digital count, with an important contribution from digitization error, but also is affected heavily by the mathematical expression used to predict the value of the dependent variable, because both the independent and the dependent variables contain random noise. In addition, model errors have a major impact on the uncertainties of the coefficients. The Maximum Likelihood approach demonstrates the inadequacy of the attenuation method model with a quadratic polynomial for the retrieved spectral radiance. We show that using the inadequate model dramatically increases the uncertainties of the coefficients. We compute the coefficient values and their uncertainties, considering both measurement and model errors.

Keywords: remote sensing, radiance, calibration, maximum likelihood, model inadequacy, VIIRS, MODIS, least-squares

1. INTRODUCTION

As the next generation remote sensing optical instrument to the MODerate Resolution Imaging Spectroradiometer[1] (MODIS), a VIIRS instrument[2] will be carried aboard each platform of the Joint Polar Satellite System and the National Polar-orbiting Environmental Satellite System Preparatory Project (NPP). The VIIRS instrument offers high quality imaging capabilities in visible and infrared bandwidths with slightly finer spatial resolution than the MODIS', providing more accurate global weather and environmental data. Due to limited on-orbit calibration means, to accurately measure the detected spectral radiance, extensive prelaunch efforts have been conducted to calibrate and characterize the sensors.

To facilitate aperture spectral radiance determination, we assume that the radiance relates a sensor's DN count through a mathematical expression. In order to gain robustness and accuracy, extending the linear mathematical form used in the MODIS for RSB and taking the similar expression used for both the MODIS and VIIRS Thermal Emissive Bands[3, 4], we use a quadratic polynomial for the radiance

$$L_{\text{det}} = c_0 + c_1 dn + c_2 dn^2 , \tag{1}$$

where dn is the background subtracted Digital Number. The polynomial coefficients are determined pre-launch, using a National Institute of Standards and Technology (NIST) traceable Spherical Integrating Source (SIS-100). Because the SIS-100 light source is not stable enough over time and its output radiance is not accurately known with a relative uncertainty of a few percent, an attenuation method is applied to determine the c-ratios: c_0 / c_1 and c_2 / c_1.

In the attenuation method, the sensor measures the same output radiance of SIS-100 with and without an attenuator . Since the time duration between reading the digital counts is short (2-3 minutes), it is reasonable to assume that the SIS-100 output radiance does not change much in the time duration. Because the attenuator is an opaque plate with small holes to allow light through, the attenuator's transmittance is unchanged over the entire SIS-100 output radiance levels. Consequently, the ratio of the detected spectral radiances with and without the attenuator may be described by

$$\tau = \frac{c_0 / c_1 + dn_{\text{in}} + (c_2 / c_1) dn_{\text{in}}^2}{c_0 / c_1 + dn_{\text{out}} + (c_2 / c_1) dn_{\text{out}}^2} , \tag{2}$$

where dn_{in} and dn_{out} denote the dn with and without the attenuator, respectively, and τ the transmittance, a constant across lamp levels. The c-ratios are determined through Eq. (2).

The legacy approach to determine the c-ratios uses a least-squares process with equal weights, namely, each data point in the least-squares has the same weight. This approach can be problematic, especially when most of the measurement data points are poorly determined, resulting in inaccurate values for the parameters. In addition, the equal-weight approach does not give information on whether the model Eq. (2) is adequate.model is correct. An inadequate model, if forced to be used, will have a significant impact on the fitting parameters.

To address the problems of the legacy approach, in this study, we use a Maximum Likelihood[5] approach. The Maximum Likelihood assigns appropriately more weight to those data points with smaller measurement uncertainties so that with the determined c-ratios the likelihood of observing the data is at its maximum. Unlike the equal-weight approach, the Maximum Likelihood approach gives us a condition to determine the validity of the model with a very high probability. If the model is inadequate, we shall calculate the impact on the c-ratios due to the inadequacy.

In the next section, we provide our theoretical description of using the Maximum Likelihood to determine the c-ratios. We describe a method for computing c-ratio errors due to model inadequacy. In Section 3, we give an example of the results obtained by applying the theories developed in Section 2 to VIIRS FU1 Thermal Vacuum (TV) data for RSB. We use the results to determine whether the quadratic polynomial model Eq. (2) adequately describes our data. In Section 4, we try to gain insight for the procedure given in Section 2. Specifically, we consider the impact of model inadequacy on fitting parameter uncertainties. Finally, in Section 5 we summarize the results of this study.

2. MAXIMUM LIKELIHOOD APPROACH

To use existing data regression functions, we need to write Eq. (2) into a form of $y = f(x; p)$, where all the fitting parameters are represented by p. Let $x = dn_{\text{out}}$ and $y = dn_{\text{in}}$, Eq. (2) can be written as

$$y = \frac{2\left(\tau \times z - c_0 / c_1\right)}{1 + \sqrt{1 + \frac{4c_2}{c_1} \times \left(\tau \times z - c_0 / c_1\right)}} \ , \tag{3}$$

where $z = c_0 / c_1 + x + \left(c_2 / c_1\right)x^2$. The background DN is averaged over 48 consecutive Half Angle Mirror (HAM) angular positions (denoted as the sample positions) over the Space View port for each HAM side and each scan, and the Earth View DN is the average over 25 scans with repeated 3-sigma outlier rejections at each of the 120 angular positions (since a 3-sigma rejection changes the mean as well as its standard deviation, it is necessary to run the 3-sigma rejection repeatedly until the final results stabilize). Due to the DN digitization, a zero standard deviation of the mean is possible. When a zero standard deviation occurs, we assign a quantization error as the standard deviation of the averaged DN.

Even if the model is accurate, Eq. (3) may not hold due to measurement errors in *y* and/or *x*. The errors in *y* and/or *x* make the Maximum Likelihood approach viable and the weight is the inverse of the variance of $y - f\left(x; p\right)$ where $f\left(x; p\right)$ stands for the mathematical expression on the right hand side of Eq. (3) and *p* denotes the c-ratios.

In order to compute the Maximum Likelihood weight, we assume that the measurement errors follow Gaussian distributions. As a result, the probability distribution for $y - f\left(x; p\right)$ is also Gaussian. The variance of $y - f\left(x; p\right)$ is computed by

$$\sigma^2 = \mathrm{var}\left(y\right) + \mathrm{var}\left(f\left(x; p\right)\right) - 2\mathrm{covar}\left(y,\ f\left(x; p\right)\right) \ . \tag{4}$$

Since the errors in dn_{in} and dn_{out} are not correlated and $f\left(x; p\right) \approx \tau \times dn_{\mathrm{out}}$, Eq. (4) is simplified to become

$$\sigma^2 = \sigma^2\left(dn_{\mathrm{in}}\right) + \tau^2\sigma^2\left(dn_{\mathrm{out}}\right) \ . \tag{5}$$

Eq. (4) indicates that the weight in the Maximum Likelihood approach depends on the mathematical form of the fitting function.

In order to avoid any adverse effects on the determined c-ratios from the variation of the attenuator's transmittance over sample positions, we carry out our fitting procedure at each sample position. The detailed procedure is described in the following steps.

(a) At each sample position, the measured data points are denoted as $\left(dn_{\mathrm{in}}, dn_{\mathrm{out}}\right)_{\mathrm{sample}}$, for all valid SIS-100 radiance levels. Using a data regression procedure, we find the parameters $\left(c_0 / c_1, c_2 / c_1\right)_{\mathrm{sample}}$ which minimize

$$\sum_{n=1}^{N} \left[dn_{\mathrm{in}}\left(n\right) - f\left(dn_{\mathrm{out}}\left(n\right); p\right)\right]^2 / \sigma^2\left(n\right) \ ,$$

where *N* is the number of SIS-100 radiance levels. The data regression procedure we use is the Interactive Data Language function MPFIT(…)[6] which performs a Levenberg-Marquardt least-squares procedure with additional features such as allowing setting limits on the values of fitting parameters. We use repeated 4-sigma rejections until the rejection stabilizes.

(b) We determine the simple means of $(c_0/c_1, c_2/c_1)_{\text{sample}}$ over the sample positions with repeated 3-sigma outlier rejections for a set of 120 2-element vectors. At this stage, the means of $(c_0/c_1, c_2/c_1)_{\text{sample}}$ are for a single HAM side.

(c) Because the c-ratios in VIIRS RSB are not HAM side dependent (assuming the mirror does not contribute to inter-detector cross talks), we compute the simple mean of $\langle c_0/c_1, c_2/c_1\rangle_{\text{sample}}$ over HAM sides to obtain $\langle c_0/c_1, c_2/c_1\rangle_{\text{sample, HAM}}$.

At the end of step (c), we must address the question of whether the quadratic model is adequate. If the model is adequate, we can determine the covariance matrix for the c-ratios in step (b) (from the 120 c-ratio covariance matrixes). If the model is inadequate, indicated by small goodness-of-fit numbers, we have three choices to improve our capability to determine the aperture radiance. One is to change the model. Another is to divide the fitting region into two or more smaller ones and carry out the fitting process separately in those regions. The third is to apply the inadequate quadratic polynomial for the entire region, in order not to increase algorithm complexity.

Using an inadequate model can generate large differences over some radiance regions between the measured and the fit-obtained values in τ. The large differences in τ can be quantified by the variance of τ. This variance enlarges the uncertainties of $(c_0/c_1, c_2/c_1)_{\text{sample, HAM}}$. Details to compute these uncertainties are described in step (d).

(d) We denote the simple mean of the τ differences over samples and HAM sides at a particular radiance level as $\langle\Delta\tau\rangle_{\text{sample, HAM, rad}}$. $\langle\Delta\tau\rangle_{\text{sample, HAM, rad}}$ is the sum of the differences induced from random noise and model inadequacy, namely

$$\langle\Delta\tau\rangle_{\text{sample, HAM, rad}} = \langle\Delta\tau\rangle_{\text{sample, HAM, rad, noise}} + \Delta\tau_{\text{model, rad}} \quad . \tag{6}$$

Since $\Delta\tau_{\text{model, rad}}$ and $\langle\Delta\tau\rangle_{\text{sample, HAM, rad, noise}}$ are statistically independent, Eq. (6) gives

$$\left\langle\left(\langle\Delta\tau\rangle_{\text{sample, HAM, rad}}\right)^2\right\rangle = \left\langle\left(\langle\Delta\tau\rangle_{\text{sample, HAM, rad, noise}}\right)^2\right\rangle + \left(\Delta\tau_{\text{model, rad}}\right)^2 \quad , \tag{7}$$

where

$$\left\langle\left(\langle\Delta\tau\rangle_{\text{sample, HAM, rad, noise}}\right)^2\right\rangle = \eta \times \frac{\tau^2\ \text{var}(dn_{\text{out}}) + \text{var}(dn_{\text{in}})}{N_{\text{sample}} * dn_{\text{out}}^2} \quad . \tag{8}$$

In Eq. (7), η is a positive number, equal to 1 if the digital counts from consecutive samples from the same scan are not correlated. To determine η, we can average the digital counts over the samples first and then take the scan average. In Eq. (8), on the left hand side, the outer <…> indicates the statistical average and $N_{\text{sample}} = 120$.

To compute the variance in τ over the entire radiance range, we realize that the contributions to the variance from the random noise and the model errors depend differently on the number of radiance levels. The contribution from the random noise is

$$\text{var}_{\text{noise}}(\tau) = 1/\sum_{n=1}^{N} 1/\left\langle\left(\langle\Delta\tau\rangle_{\text{sample, HAM, rad, noise}}\right)^2\right\rangle \quad , \tag{9}$$

which is roughly proportionally to 1/*N*, indicating that as long as we have enough number of radiance levels, the contribution to the variance of τ can be very small. The model error generated τ difference, however, contributes to the τ variance in a mean squared fashion. Therefore, when model errors dominate, we can compute the overall τ variance as

$$\mathrm{var}(\tau) = \mathrm{var}_{\mathrm{model}}(\tau) + \mathrm{var}_{\mathrm{noise}}(\tau) \ , \tag{10}$$

where the model error created τ variance $\mathrm{var}_{\mathrm{model}}(\tau)$ is defined as

$$\mathrm{var}_{\mathrm{model}}(\tau) = \int_{L_{\min}}^{L_{\max}} \mathrm{var}_{\mathrm{model}}(\tau, L) dL / (L_{\max} - L_{\min}) \ . \tag{11}$$

In Eq. (11), the model error created variance of τ at radiance L is

$$\mathrm{var}_{\mathrm{model}}(\tau, L) = \begin{cases} \left(\langle \Delta\tau \rangle_{\mathrm{sample,\,HAM,\,rad}}\right)^2 - \left\langle \left(\langle \Delta\tau \rangle_{\mathrm{sample,\,HAM,\ rad,\ noise}}\right)^2 \right\rangle; & \text{when } \left(\langle \Delta\tau \rangle_{\mathrm{sample,\,HAM,\,rad}}\right)^2 \geq \left\langle \left(\langle \Delta\tau \rangle_{\mathrm{sample,\,HAM,\ rad,\ noise}}\right)^2 \right\rangle \\ 0; \ \text{elsewhere} \end{cases} \ . \tag{12}$$

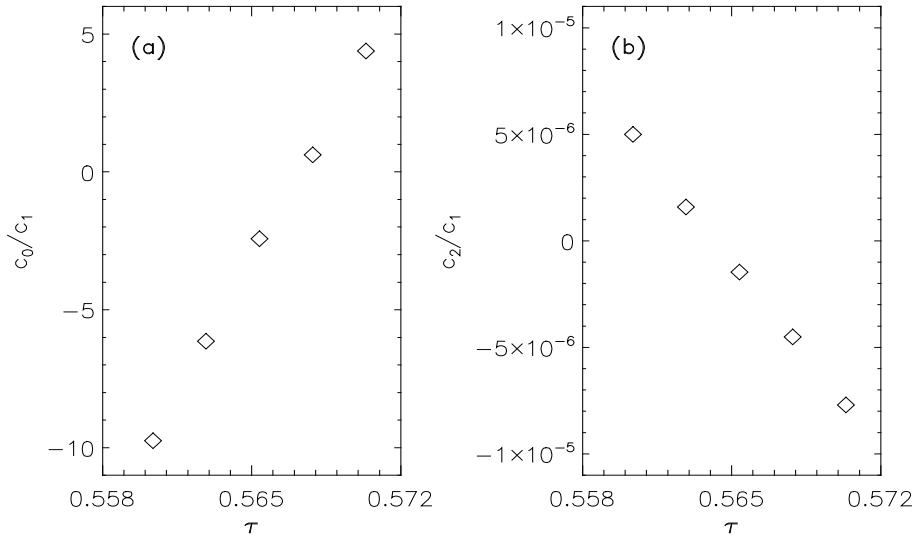

Fig. 1. Each data point is from a fit of Eq. (3) to measurement data at a fixed attenuator transmittance. (a) c_0 / c_1 versus τ. (b) c_2 / c_1 versus τ. Results are for detector 1 of band M1 at (HAM side A, Fixed High Gain, Nominal temperature plateau, control electronics side B).

To use the variance of τ to compute the uncertainties of $(c_0 / c_1, c_2 / c_1)$, we rely on the findings between the changes in (c_0 / c_1 , c_2 / c_1) and the change in τ . Mathematically, the relations can be visualized through Eq. (2) which gives that the impact of a small change in τ on the c-ratios obeys the following relation

$$\delta\tau \approx \frac{1-\tau}{dn_{\mathrm{out}}} \delta\left(\frac{c_0}{c_1}\right) + \delta\left(\frac{c_2}{c_1}\right) \times \tau \times dn_{\mathrm{out}} \times (\tau - 1) \ . \tag{13}$$

Eq. (13) demonstrates that for a small change in τ at a particular radiance level, the changes in the c-ratios fall on a straight line. Taking account all the radiance levels, in a minimum error sense, such as least-squares, we find the changes in the c-ratios due to a small change in τ behave as $\delta(c_0/c_1) \propto \langle dn_{\text{out}} \rangle \times \delta\tau$ and $\delta(c_2/c_1) \propto -\delta\tau / \langle dn_{\text{out}} \rangle$. To visually show the relation between the change in τ and the changes in the c-ratios, we use Eq. (3) and carry out data regressions at a few fixed τ at sample position one for detector 1 of band M1 (412 nm) at (HAM side A, Fixed High Gain, Nominal temperature plateau, control electronics side B). Figs. 1a and 1b show plots for c_0/c_1 versus τ and c_2/c_1 versus τ, respectively. The figures clearly indicate linear relationship between the c-ratios and τ. As a result, we compute the uncertainties of the c-ratios by multiplying the square root of $\text{var}(\tau)$ by the absolute values of the slopes exhibited by the data points in Figs. 1a and 1b, respectively. Furthermore, the figures reveal that if model error dominates over the random measurement errors, the correlation coefficient for the c-ratios is -1.

That we are interested in the variances of the c-ratios is because we want to determine the relative uncertainty of $c_0/c_1 + dn + c_2/c_1 \times dn^2$, computed by

$$\frac{std\left(\frac{c_0}{c_1} + dn + \frac{c_2}{c_1} \times dn^2\right)}{\frac{c_0}{c_1} + dn + \frac{c_2}{c_1} \times dn^2} = \frac{\sqrt{\text{var}\left(\frac{c_0}{c_1}\right) + \text{var}(dn) \times \left(1 + 2dn \times \left(\frac{c_2}{c_1}\right)\right)^2 + \text{var}\left(\frac{c_2}{c_1}\right) \times dn^4 + 2dn^2 \times \text{covar}\left(\frac{c_0}{c_1}, \frac{c_2}{c_1}\right)}}{\frac{c_0}{c_1} + dn + \frac{c_2}{c_1} \times dn^2}. \quad (14)$$

3. RESULTS

We carry out the steps mentioned in Section 2 and obtain the results for all detectors in RSB, at electronics gain settings of Fixed Low and High Gains, for temperature plateaus of Cold, Nominal and Hot, and at control electronics sides A and B, using VIIRS TV RC-02 data. The values of the c-ratios agree with those obtained previously with the equal-weight approach within the standard deviations from the equal-weight approach.

To determine the c-ratio variances and the correlation coefficient, after we carry out the data regression at the per sample stage, we compute the chi-square and the chi-square at goodness-of-fit of 0.001. The chi-squares for detector 1 of band M1 at (Fixed High Gain, Nominal temperature plateau, control electronics side B) are about 250 for all the samples and HAM sides, significant larger than 145 which is about the chi-square at goodness-of-fit of 0.001, indicating strongly that the quadratic model is inadequate. We therefore use step (d) to compute the variances of the c-ratios through the variance of τ and assign -1 to the c-ratio correlation coefficient.

In Figs. 2a and 2b, we show our results in diamonds for the c-ratios and their standard deviations for the detectors in band M1 at (HAM side A, Fixed High Gain, Nominal temperature plateau, control electronics side B). In the figures, error bars stand for the standard deviations. The squares are for the equal-weight approach without considering model errors. For the Maximum Likelihood approach without considering model errors, namely without step (d), the standard deviations for the c-ratios are about an order of magnitude smaller than the ones from the equal-weight approach. After considering model errors, the standard deviations for the c-ratios increase dramatically as shown in the figures.

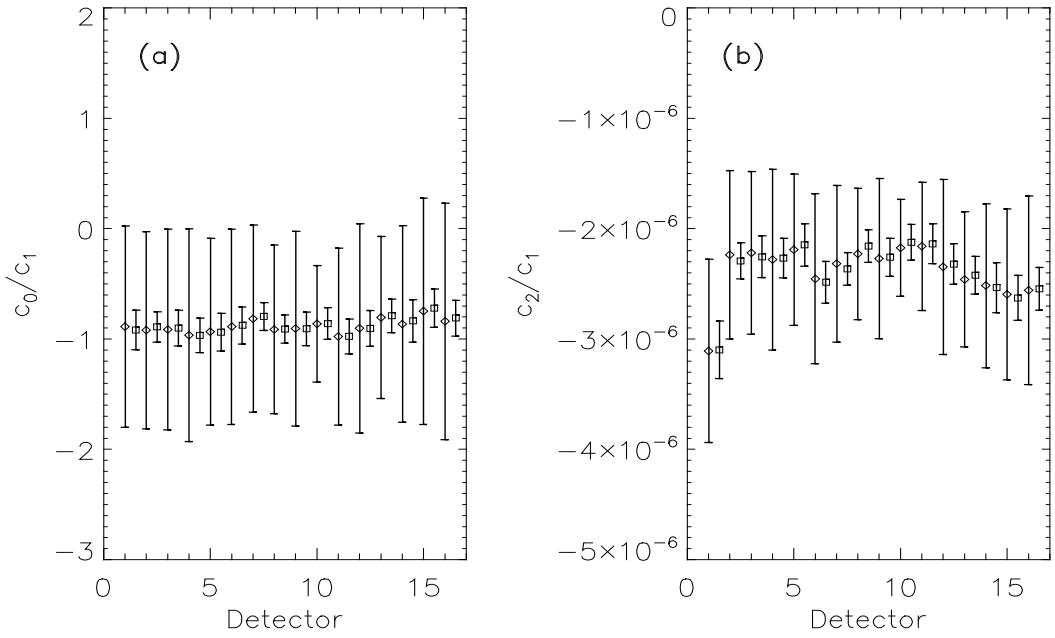

Fig. 2. Diamonds are for HAM and sample averaged (simple average) c-ratios from the Maximum Likelihood fits of Eq. (3) to measurement data for all detectors in band M1 at Fixed High Gain and Nominal temperature plateau at control electronics side B. Bars stand for the standard deviations. Squares are for the equal-weight approach. (a) c_0/c_1. (b) c_2/c_1.

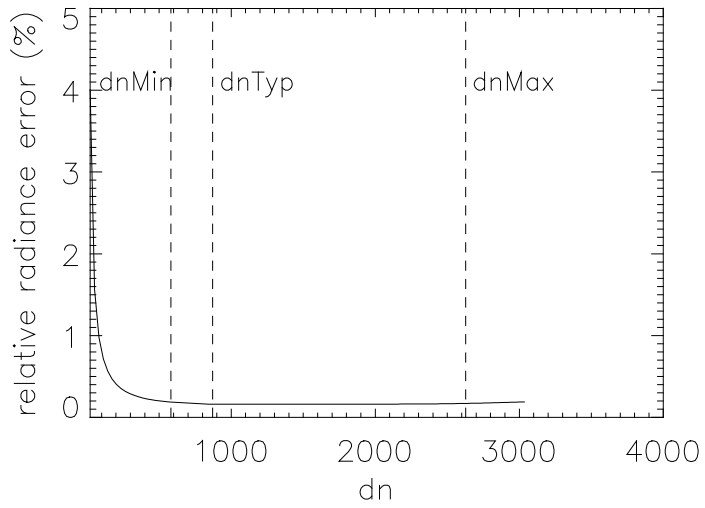

Fig. 3. Relative radiance errors, in percentage, computed from Eq. (13) for band M1 detector 1, at (HAM side A, Fixed High Gain, Nominal temperature plateau, control electronics side B).

With the variances and the covariance of the c-ratios, we compute the relative radiance errors, determined by Eq. (14). We show the results in Fig. 3 for detector 8 in band M1 at (HAM side A, Fixed High Gain, Nominal temperature plateau, control electronics side B). The dashed vertical lines indicate the dn at the requirement

specified minimum, typical, and maximum radiances. From the figure, we can see that the relative error is quite small (less than 0.3%) over $[L_{\min}, L_{\max}]$. When *dn* becomes smaller than 300 (<dnMin)), with decreasing *dn*, the relative error becomes larger quickly.

4. DISCUSSION

To justify the Maximum Likelihood approach and the application of Eq. (10) to compute the variance of τ in the case of model inadequacy, we consider fitting the model of a constant. We assume that at $\{x_m; m = 1, \cdots, M\}$, the measured value set is $\{y_m\}$. With a measurement error δy_m and a bias function $b(x)$, we have the following equation relating the measurement value with the true value

$$y_m = C + b(x_m) + \delta y_m \ . \tag{15}$$

The Maximum Likelihood approach yields that

$$C = \frac{\sum_{m=1}^{M} [y_m - b(x_m)] / \sigma_m^2}{\sum_{m=1}^{M} 1/\sigma_m^2} \ . \tag{16}$$

We force a constant model of

$$y_m = C' + \delta_m \tag{17}$$

by removing the bias function to obtain

$$C' = \frac{\sum_{m=1}^{M} y_m / \sigma_m^2}{\sum_{m=1}^{M} 1/\sigma_m^2} \ . \tag{18}$$

Comparing Eqs. (16) and (18), we know

$$C = C' - \frac{\sum_{m=1}^{M} b(x_m) / \sigma_m^2}{\sum_{m=1}^{M} 1/\sigma_m^2} \ . \tag{19}$$

Given Eqs. (15-19), the question we need to answer is how we can use the fit-obtained *C'* to predict the true $C + b(x)$ with some level of certainty.

We can see from Eq. (19) that *C* and *C'* differ by the weighted sum of the biases $\sum_{m=1}^{M} b(x_m)/\sigma_m^2 \ / \sum_{m=1}^{M} 1/\sigma_m^2$. Although we do not exactly know the bias function, it can be computed approximately. If model errors dominate measurement errors, indicated by a very small goodness-of-fit number, we can replace $b(x_m)$ by $y_m - C'$ and obtain

$$\frac{\sum_{m=1}^{M} b(x_m)/\sigma_m^2}{\sum_{m=1}^{M} 1/\sigma_m^2} = 0 \ . \tag{20}$$

Therefore, C and *C'* essentially are the same.

Next, we need to find the standard deviation of *C'* in the presence of biases. Assuming $\text{covar}(y_i, y_j; i \neq j) = 0$, the variances of *C'* from the random noise is computed by

$$\text{var}_{\text{noise}}(C') = \frac{1}{\sum_{m=1}^{M} 1/\sigma_m^2} \ , \tag{21}$$

indicating that the variance of *C'* from measurement errors can be very small, as long as we have enough number of data points. Consequently, Eq. (21) can not address the effect of the biases since the biases are not random and more data points should not decrease the variance of *C'*. As a result, in the presence of biases, obtaining the variance from the output covariance matrix generated by data regression routines will not be correct, whether to use Maximum Likelihood weights or a uniform weight. With biases, the variance of *C'* may be computed by

$$\text{var}(C') = std^2(b) + \text{var}_{\text{noise}}(C') \ . \tag{22}$$

$std(b)$ is defined as that over $[x_{\min}, x_{\max}]$, 68.2% of $|b(x)|$ are smaller than $std(b)$. Eq. (22) may be approximated by

$$\text{var}(C') = \int_{x_{\min}}^{x_{\max}} b^2(x)dx/(x_{\max} - x_{\min}) + \text{var}_{\text{noise}}(C') \ . \tag{23}$$

Since we do not exactly know the bias function, to compute the variance of *C'*, Eq. (23) is approximated by

$$\text{var}(C') = \text{var}_{\text{model}}(C') + \text{var}_{\text{noise}}(C') \ , \tag{24}$$

where $\text{var}_{\text{model}}(C')$ is defined by

$$\text{var}_{\text{model}}(C') = \int_{x_{\min}}^{x_{\max}} \text{var}_{\text{model}}(C', x)dx/(x_{\max} - x_{\min}) \ , \tag{25}$$

and

$$\text{var}_{\text{model}}(C', x) = \begin{cases} (y - C')^2 - \sigma_m^2; & \text{when } (y - C')^2 \geq \sigma_m^2 \\ 0; & \text{otherwise} \end{cases} \ . \tag{26}$$

With *C'* obtained by Eq. (18) and its variance given by Eq. (24), for a particular measurement at *x*, if the model is inadequate, we can state that, with about 68.2% confidence, the true value $C + b(x)$ resides in the region of $\left[C' - \sqrt{\text{var}(C')}, C' + \sqrt{\text{var}(C')}\right]$.

As an example to illustrate our theoretical results developed in this section, we fit our model Eq. (17) to a measured data set of $y = 0.01\times x^2 + Norm(1)$ in the x region of $[-25, 25]$, where $0.01\times x^2$ is the true value and $Norm(1)$ is the measurement error which is Gaussian distributed with a Gaussian width of one. We use both the equal-weight and the Maximum Likelihood approaches with the number of data points of 51 and 201 respectively.

In Figs. 4c and 4d, we show our fitting results, along with the fitting results from the equal-weight approach shown in Figs. 4a and 4b. In the figures, the diamonds represent te measurement data, the dashed lines for the real values of the data, and the solid lines for the fitting results with the bars indicating the standard deviations of the fit-obtained *C'*. Figs. 4a and 4b show that the standard deviations obtained from the equal-weight approach are unrealistically too small, whereas the standard deviations in Figs. 4c and 4d are about correct demonstrated by $C'\pm std(C')$ covering slightly more than half of the real values.

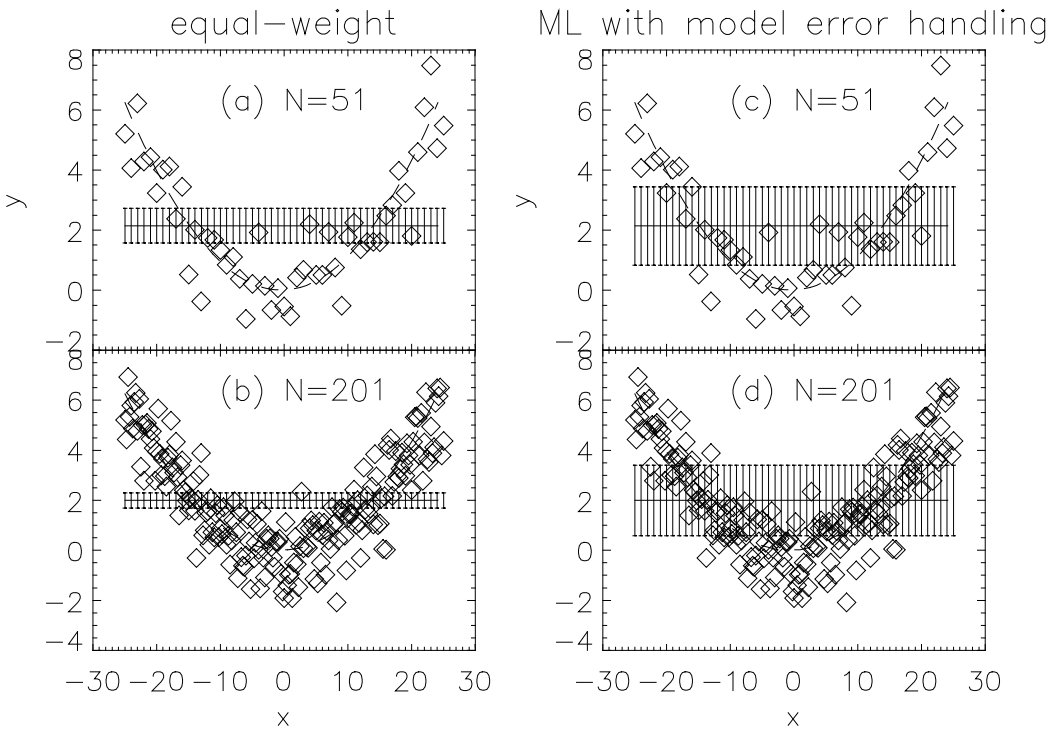

Fig. 4. Fits of Eq. (17) to $0.01x^2 + Norm(1)$ over the x range of [-25, 25], using the equal-weight and Maximum Likelihood approaches, respectively with the number of data points of N=51 and N=201. (a-b) Equal-weight approach. (c-d) Maximum Likelihood approach with model error handling.

For a future study, we would like to extend our simple model Eq. (17) to more complicated ones and compute the effects of model errors to the coefficients in those models. It is also desirable to compute $std(b)$ more accurately.

5. SUMMARY

In this proceeding, we showed a Maximum Likelihood approach to determine the c-ratios in the quadratic polynomial detector spectral radiance model. We gave mathematical expressions to compute the weights used in the approach, considering the random noises from both the dependent and independent variables. In addition, we developed a methodology to compute the impact of model errors on the c-ratios. We applied our Maximum Likelihood method to the VIIRS RSB measurement data. Our results revealed that the obtained c-ratios are in good agreement with those computed with the equal-weight method even though the quadratic model is may not be inadequate over the radiance range specified by the requirement. Critical to the knowledge of the measured radiance error, our Maximum Likelihood with model error handling approach yielded much more realistic c-ratio variances that are much larger than those from the data regression generated covariance matrix. We pointed out that because the biases are not random numbers, the uncertainties of the fitting parameters can not be reduced simply by fitting more data points. Therefore, in the presence of significant model errors, the covariance matrix values from data regression routines incorrectly address the variances of the fitting parameters. The Maximum Likelihood approach shown in this proceeding may lead to better sensor calibration, including better understanding of sensor calibration uncertainty.

ACKNOWLEDGEMENTS

We would like to thank Frank DeLuccia and Kameron Rausch of the Aerospace Corporation for useful discussions. We also want to thank the Raytheon El Segundo team for providing VIIRS test data and the Northrop Grumman team for their support in the testing and data analysis improvements. This study is supported by NASA funding for NPP Instrument Calibration Support Element (NICSE).

REFERENCES

[1] Xiong, X., Sun, J., Barnes, W., Salomonson, V., Esposito, J., Erives, H., and Guenther, B., “Multiyear On-Oribt Calibration and Performance of Terra MODIS Reflective Solar Bands”, IEEE Trans. Geosci. Remote Sens., Vol. 45(4), 879-889 (2007).

[2] Butler, J., Xiong, X., Oudrari, H., Pan, C., and Gleason, J., “NASA Calibration and Characterization in the NPOESS Preparatory Project (NPP)”, IGARSS, July 12-17, 2009, Cape Town, South Africa.

[3] Xiong, X. and Barnes, W., “Early On-orbit Calibration Results from Aqua MODIS”, Proc. SPIE Vol. 4881, 327-336 (2003).

[4] Guenther, B., Godden, D., Xiong, X., Knight, E. J., Qiu, S. Y., Montgomery, H., Hopkins, M. M., Khayat, M. G., and Hao, Z., “Prelaunch Algorithm and Data Format for the Level 1 Calibration Products for the EOS-AM1 Moderate Resolution Imaging Spectroradiometer (MODIS)”, IEEE Trans. Geosci. Remote Sens., Vol 36(4), 1142-1151 (1998).

[5] Press, W., Teukolsky, S. A., Vetterling, W. T., and Flannery, B. P., [Numerical Recipes], Cambridge University Press, New York, (776-787) 2007.

[6] Markwardt, C. B., “Non-linear Least Squares Fitting in IDL with MPFIT”, Proc. Astro. Data Analysis Software and Sys. XVIII, ASP Conference Series, Vol. 411, 251-254 (2008).

* ning.lei@sigmaspace.com

APPENDIX

In this appendix, in order to evaluate our results given in this proceeding, we shall carry out a computer simulation to generate dn_{in} and dn_{out}. We then and fit the simulated data to extract the c-ratios and their variances, following the procedure described in Section 2. The simulation assumes that the true radiance, after divided by c_1, follows a cubic polynomial in *dn*:

$$\frac{L_{true}}{c_1} = \frac{c_0}{c_1} + dn + \frac{c_2}{c_1} \times dn^2 + \frac{c_3}{c_1} \times dn^3 \quad . \tag{A.1}$$

In the simulation, we set $c_0 / c_1 = -0.85$, $c_2 / c_1 = -3 \times 10^{-6}$, $c_3 / c_1 = -1.6 \times 10^{-9}$, and $\tau = 0.566$. The results are shown in Fig. A1 and Fig. A2. From Fig. A1, we can see that the Maximum Likelihood approach fit-obtained τ (shown by the solid horizontal line) is much different from the true τ. Fig. A2(a) shows the results from applying the Maximum Likelihood method with model error handling. Fig. A2(b) shows the results from the equal-weight approach. The large difference between the retrieved and the true radiances is indicative of flaws in the attenuation method used in this study.

To resolve the large difference between the retrieved and the true radiances, shown in Fig. A2, we carry out fits with the attenuator's transmittance fixed at its true value of 0.566. The results are shown in Figs. A3 and A4. From Fig. A4, we can see that in this case the retrieved radiances are much closer to the real ones, indicating that we may need to know the attenuator's transmittance before using the attenuation method.

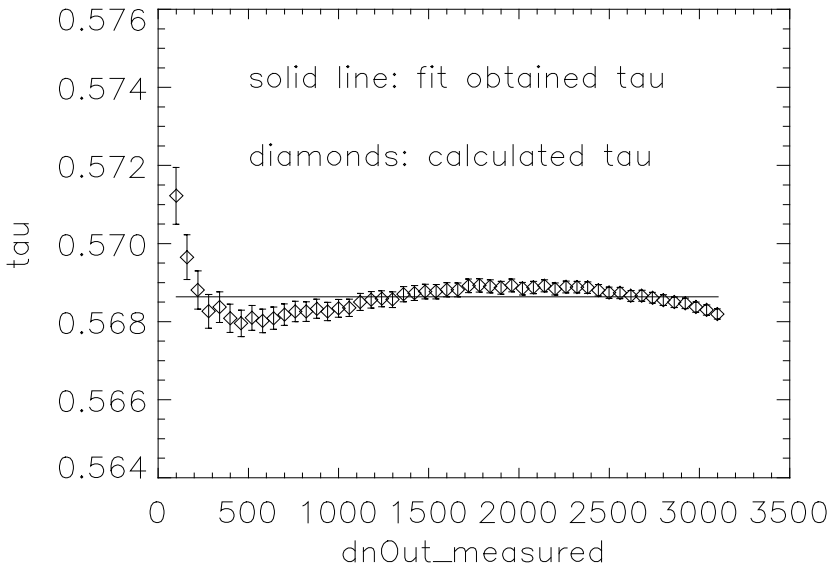

Fig.A1. Results from the fits to simulated data, following the procedure in Section 2. Diamonds are calculated τ and the horizontal solid line is for the fit-obtained τ from the Maximum Likelihood approach.

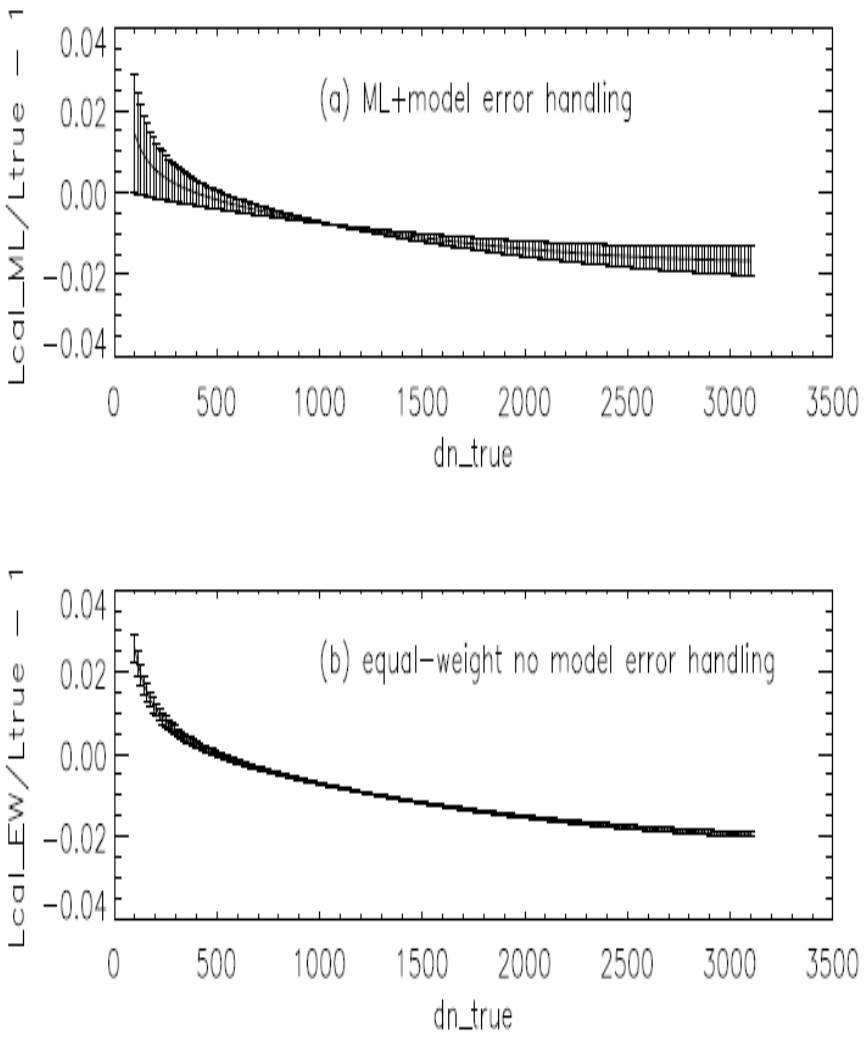

Fig.A2. The ratio of the retrieved radiance over the true radiance minus one. (a) Maximum Likelihood approach. (b) Equal-weight approach.

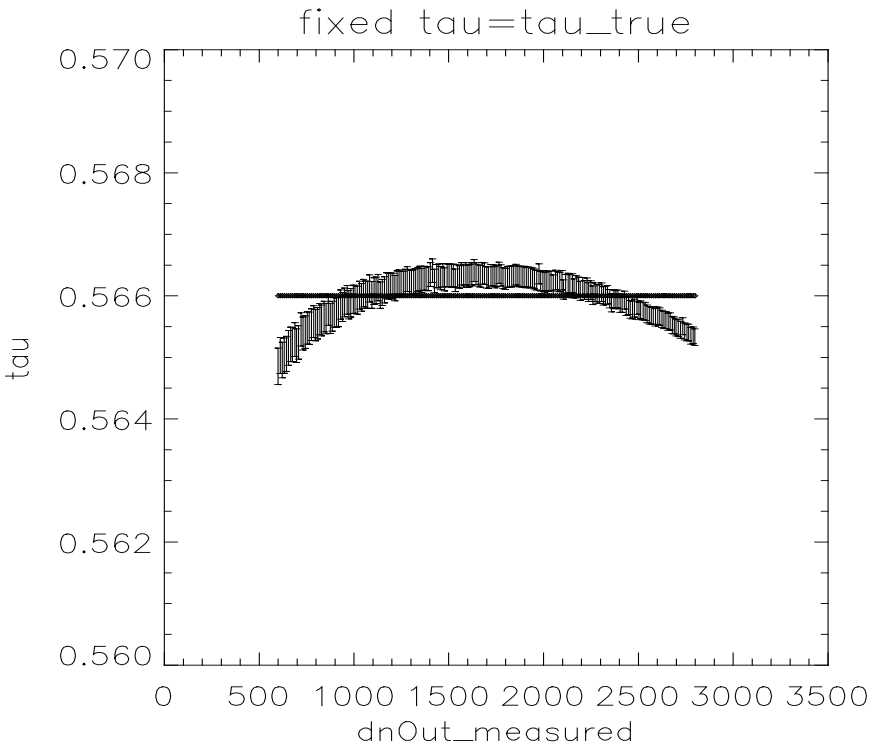

Fig.A3. Results from the fits to simulated data, with τ fixed at 0.566. Diamonds are calculated τ and the horizontal solid line is for the fit-obtained τ from the Maximum Likelihood approach.

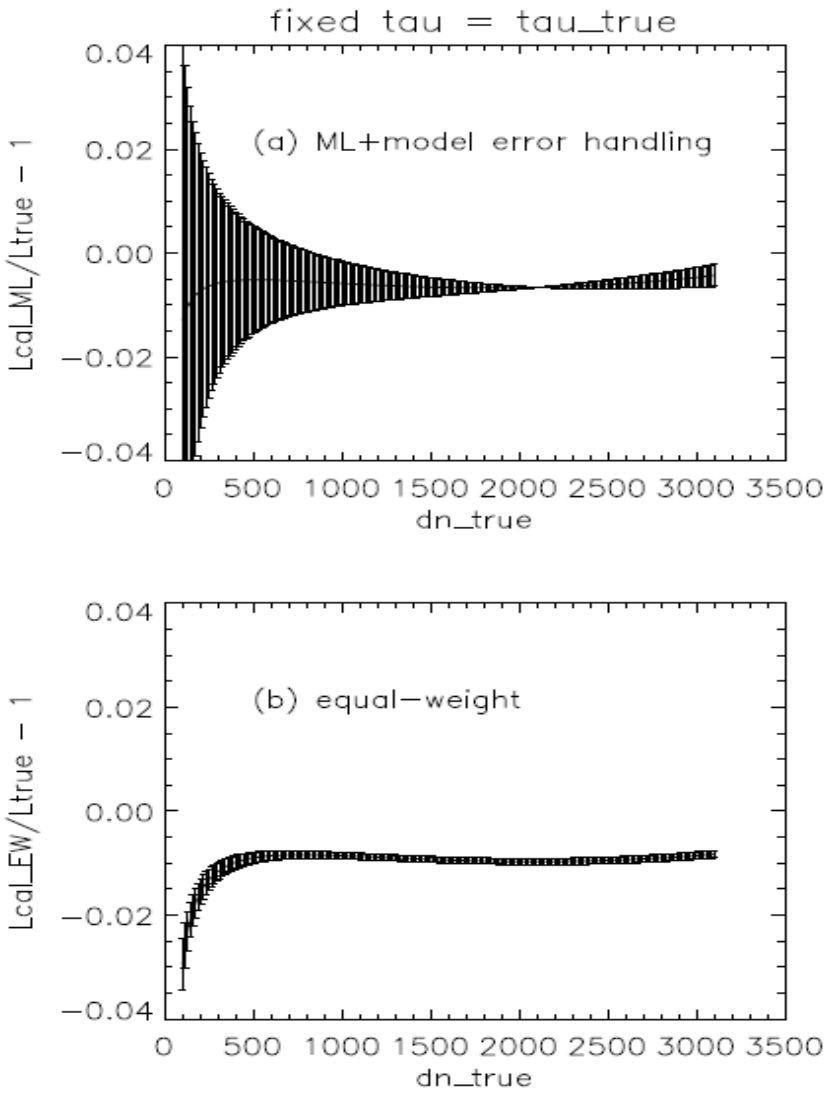

Fig.A4. The ratio of the retrieved radiance over the true radiance minus one at $\tau = 0.566$. (a) Maximum Likelihood approach. (b) Equal-weight approach.

to